# *Staphylococcal* sRNA IsrR down-regulates methylthiotransferase MiaB under iron-deficient conditions

Maxime Barrault[1], Elise Leclair[1], Eric Jacquet[2] and Philippe Bouloc[1#]

[1]Université Paris-Saclay, CEA, CNRS, Institute for Integrative Biology of the Cell (I2BC), 91198 Gif-sur-Yvette, France

[2]Université Paris-Saclay, CNRS, Institut de Chimie des Substances Naturelles, UPR2301, 91198 Gif-sur-Yvette, France

N° ORCID:

- Maxime Barrault: 0000-0003-3949-7598
- Elise Leclair: 0009-0000-3706-6554
- Eric Jacquet: 0000-0001-6366-8436
- Philippe Bouloc: 0000-0003-4601-3387

[#]Correspondence: philippe.bouloc@i2bc.paris-saclay.fr

**Running title:** Staphylococcal sRNA IsrR down-regulates *miaB*.

**Keywords**: *Staphylococcus aureus*, IsrR, iron homeostasis, [Fe-S] clusters, small regulatory RNA, translational regulation.

## ABSTRACT

*Staphylococcus aureus* is a major contributor to bacterial-associated mortality, owing to its exceptional adaptability across diverse environments. Iron, vital for most organisms, poses toxicity risks in excess. To manage iron, *S. aureus*, like many pathogens, employs intricate systems. We have recently identified IsrR as a key regulatory RNA induced during iron starvation. Its role is to reduce the synthesis of non-essential iron-containing proteins under iron-depleted conditions. In this study, we unveil IsrR's regulatory action on MiaB, an enzyme responsible for methylthio group addition to specific sites on transfer RNAs (tRNAs). We use predictive tools and reporter fusion assays to demonstrate IsrR's binding to the Shine-Dalgarno sequence of *miaB* RNA, thereby impeding its translation. The effectiveness of IsrR hinges on the integrity of a specific C-rich region. As MiaB is non-essential and has iron-sulfur clusters, IsrR induction spares iron by downregulating *miaB*. This likely enhances *S. aureus* fitness and aids in navigating the host's nutritional immune defenses.


## IMPORTANCE

In many biotopes, including those found within an infected host, bacteria confront the challenge of iron deficiency. They employ various strategies to adapt to this scarcity of nutrients, one of which involves regulating iron-containing proteins through the action of small regulatory RNAs. Our study shows how IsrR, a small RNA from *S. aureus*, prevents the production of MiaB, a tRNA-modifying enzyme containing iron-sulfur clusters. Through this illustration, we shed light on a novel substrate for a small RNA-sparing iron, thereby unveiling a way by which bacteria conserve their iron resource.

## INTRODUCTION

*Staphylococcus aureus* is the leading cause of bacteria-associated mortality worldwide (1). Its pathogenicity is due to its adaptability across various biotopes and the expression of multiple virulence determinants. Iron is a trace element universally required for growth, but toxic in excess. *S. aureus*, akin to other pathogens, has elaborate systems for maintaining its intracellular iron homeostasis to match environmental conditions (2).

We recently identified and characterized IsrR, a small regulatory RNA (sRNA) of *S. aureus*, contributing to an adaptive response to iron scarcity (3). Most sRNAs exert their activity by pairing with target mRNAs whose stability and/or translation they affect. They are generally expressed conditionally and contribute to adaptation to various growth conditions. Their estimated number in *S. aureus* varies from around 50 to a few hundred according to studies. They are major regulators or contributors to fine-tune processes including metabolism, virulence, and antibiotic resistance; however, the function of most of them remains unknown (4-6).

IsrR, by restricting the production of non-essential iron-containing proteins, is expected to spare iron for indispensable functions. *isrR* expression is repressed by the ferric uptake regulator (Fur) which is active in iron-rich environments. Induced during iron deficiency, IsrR targets Shine-Dalgarno motifs on mRNAs coding for iron-containing proteins, notably restraining translation of specific mRNAs (*fdhA*, *narG*, *nasD*, and *gltB2*) linked to nitrate respiration and encoding [Fe-S] cluster-dependent enzymes (3). Given limited iron requirements, fermentative pathways are favored under iron-limited conditions. IsrR is a functional analog of RyhB from *Escherichia coli* (7) and of other sRNAs found in diverse bacterial species (reviewed in (8, 9)) sharing targets and iron regulation. However, IsrR does not share sequence similarities or the same enzymatic requirements for its activity with RyhB and its reported functional analogs. IsrR, conserved within the Staphylococcus genus, is likely not an ortholog of these sRNAs, pointing to a convergent evolutionary solution for adaptation to low-iron conditions (3).

Hosts prevent pathogen growth through an arsenal of defense mechanisms, one of which, known as nutritional immunity, is the sequestration of nutrients such as iron (10). We reported that IsrR deficiency results in reduced virulence of *S. aureus* in a murine infection model, highlighting the role of IsrR in facilitating optimal spread of *S. aureus* in the host environment, probably critical for evasion of nutritional immunity (3).

Here, we demonstrate that IsrR downregulates *miaB* encoding a non-essential protein containing [Fe-S] clusters. This new example shows that IsrR is a central player in the maintenance of iron homeostasis in *S. aureus*.

## MATERIALS AND METHODS

### Bacterial strains, plasmids and growth conditions

Bacterial strains, plasmids and primers used for this study are described in Table 1. Plasmids were engineered by Gibson assembly (11) in *E. coli* IM08B (12) as described (Table 1), using the indicated appropriate primers for PCR amplification. Plasmids were verified by DNA sequencing and then transferred into *S. aureus*. Strains carrying the chromosomal *miaB-flag* allele were constructed using pIMmiaBflag, a pIMAY (12) derivative, as described (13). Strains carrying the chromosomal reporter gene 5'*miaB*-mAm and its mutated derivative 5'*miaB(TAT)*-mAm were constructed using the pRN112 derivatives pRN112-5'miaB and pRN112-5'miaB(TAT), respectively, as described (14). The *fur*::*tet* allele was transferred by 80 phage-mediated transduction.

*S. aureus* strains were grown aerobically in Brain Heart Infusion (BHI) broth at 37°C. *E. coli* strains were grown aerobically in Luria-Bertani (LB) broth at 37°C. Antibiotics were added to media as needed: ampicillin 100 µg/ml and chloramphenicol 20 µg/ml for *E. coli*; chloramphenicol 5 µg/ml and tetracycline 2.5 µg/ml for *S. aureus*. Iron-depleted media was obtained by the addition of DIP (2,2'-dipyridyl) 0.5 mM incubated for 30 min before any use.

### Biocomputing analysis

Pairing predictions between IsrR and the mRNA targets were made using IntaRNA (15) set with default parameters except for suboptimal interaction overlap set to "can overlap in both". The sequences used for IsrR and mRNA targets were extracted from the *S. aureus* NCTC8325 strain (NCBI RefSeq NC_007795.1). For the mRNA targets, the sequences used started at the TSS when known (e.g., EMOTES (16) or were arbitrarily made to start at nucleotide -60 with respect to the +1 of translation. The sequences contain the 5' UTR and the 17 first codons of the CDS.

### Statistical tests

For Western-blots and fluorescence experiments, statistical analyses between two groups were made by testing the equality of variances between the groups using a Fisher test and, if and only if the two variances are equal, comparing them using a t-test. Error bars represent the standard deviation of the results.

### Western blot analysis

The chromosomal *miaB-flag* reporter gene was constructed as described (Table 1). Strains were grown overnight with and without DIP. Protein extracts were prepared as follows: 4 mL of the bacterial culture were harvested by centrifugation at 4°C and 3800 g for 5 min. The resulting pellet was resuspended in 400 µL of 50 mM Tris-HCl. Cell disruption was achieved

using a Fast-Prep homogenizer (MP Biomedicals). After disruption, crude protein extracts were obtained by centrifugation at 4°C and 21000 g for 15 min. The protein concentration of each extract was determined using the Bradford protein assay method. Ten µg of each protein extract were loaded onto a NuPAGE 4%-12% Bis-Tris gel (Invitrogen). Electrophoresis was carried out at 150V for 45 min. Proteins were transferred from the gel to a PVDF membrane using the iBind system (Invitrogen). Immunolabeling was performed overnight using a rabbit anti-Flag antibody (Invitrogen) as primary antibody and an anti-rabbit IgG HRP-conjugated antibody (Promega) as secondary antibody. The iBlot system (Invitrogen) was employed for antibody incubation. Images of the immunolabeled membrane were acquired using a ChemiDoc MP imaging system (Bio-Rad). Bands were quantified using the Image Lab software (Bio-Rad).

**Fluorescent translational reporter assay**

A *miaB* translational reporter ($P_{sarA}$-5'miaB-mAm) was inserted between genes *SAOUHSC_00037* and *SAOUHSC_00039* in HG003 and HG003 Δ*isrR*::*tag135* using pRN112-5'miaB (Table 1), a pRN112 derivative, as described (14). Notably, the mAmetrine reporter gene (*mAm*) was placed in-frame and downstream *miaB* 18$^{th}$ codon with the *miaB* 5'UTR placed under the control of the P1 promoter of *sarA* ($P1_{sarA}$). Subsequently, the strains carrying the reporter fusion were transformed with plasmids expressing *isrR*, along with its various derivatives featuring CRR deletions. These plasmids are pRMC2ΔR-IsrR, pRMC2ΔR-IsrRΔC1, pRMC2ΔR-IsrRΔC2, pRMC2ΔR-IsrRΔC3, pRMC2ΔR-IsrRΔC1C2, pRMC2ΔR-IsrRΔC1C3, pRMC2ΔR-IsrRΔC2C3, and pRMC2ΔR-IsrRΔC1C2C3. For fluorescence measurements, the transformed strains were cultured overnight in BHI medium supplemented with chloramphenicol and DIP. Subsequently, cultures were washed three times with 1x phosphate-buffered saline (PBS). Fluorescence levels were quantified using a microplate reader (CLARIOstar) with excitation at 425 nm and emission at 525 nm. To ensure accuracy, fluorescence measurements were normalized by subtracting the auto-fluorescence of the HG003 strain (lacking the reporter construct), and all cultures were adjusted to an optical density at 600 nm ($OD_{600}$) of 1.

**Quantitative reverse transcriptase PCR**

Overnight cultures HG003 and HG003 Δ*isrR* (biological triplicates, N=3) were diluted to an $OD_{600}$ = 0,005 and incubated in BHI supplemented with DIP (0.5 mM) at 37°C. At $OD_{600}$ = 1, rifampicin (concentration 200 µg/ml) was added to the growth medium. Bacterial cultures were harvested before rifampicin addition (time 0) and at 2, 5, and 10 min after rifampicin addition. Total RNAs were extracted as described (17) and treated with DNase (Qiagen) according to manufacturer's instructions. The last purification step was performed with the

RNA Nucleospin Kit according to manufacturer's instructions (Macherey-Nagel). The integrity of the RNAs was verified using the Agilent 2100 bioanalyzer with the RNA 6000 Nano kit (Agilent Technologies). qRT-PCR experiments and data analysis were performed as described (18). The Ct values of *rrsA* were used to normalize the data and the determination of the gene expression ratio was achieved using the $\Delta\Delta$Ct method. Primers used for qRT-PCRs are indicated in Table 1.

## RESULTS

### MiaB is a putative IsrR-target

We used CopraRNA (19), a software designed for predicting targets of bacterial sRNAs across diverse species, to unveil potential targets of IsrR. Given *isrR* conservation throughout the Staphylococcus genus, CopraRNA emerged as an efficient tool for IsrR target prediction (20), resulting in the successful validation of four of its targets as reported (3). Among the predicted targets was *miaB* mRNA (3, 21). The latter encodes MiaB, a methylthiotransferase catalyzing the addition of a methylthio group ($ms^2$) to isopentenyl adenine ($i^6A$) at position 37 ($ms^2i^6A$-37) of transfer RNA (tRNA) anticodons (22). This modification is present in most tRNAs reading codons starting with a U and is conserved from bacteria to human (23); it contributes to stabilizing the codon–anticodon interaction (24) and affects translational accuracy (25).

To substantiate the proposed interaction between IsrR and *miaB* mRNA, we used the IntaRNA software (15). The input was the complete IsrR sequence and the *miaB* 5' untranslated region (UTR) with 25 codons. IsrR is characterized by three single-stranded C-rich regions, denoted as CRR1, CCR2, and CRR3 (3). The CRRs are common sequences among Firmicutes' regulatory RNAs where they are presumably seed-binding motifs to G-rich sequences (26). IntaRNA analysis suggests a potential pairing of IsrR with the Shine-Dalgarno sequence of *miaB* RNA (Figure 1A). The pairing involves 55 nucleotides, an unusually high number of pairs. The energy of sRNA-mRNA pairing is low (-22.33 kcal/mol) supporting its existence. It involves the CCR3 GCCCG sequence, which could serve as a seed motif of the interaction. Of note, the isrR/ *miaB* mRNA pairing also is conserved within the Staphylococci genus (Figure 1B).

### IsrR-dependent reduction of MiaB expression

To explore the potential influence of IsrR on *miaB* expression, a gene fusion was constructed wherein the native *miaB* gene was replaced by a copy harboring the complete *miaB* open reading frames extended with a C-terminal Flag sequence (Figure 2A). The resulting MiaB-Flag fusion protein was detectable through anti-Flag antibodies, thereby serving as a quantifiable surrogate for wild-type gene expression levels. This reporter fusion was integrated into the chromosomes of both HG003 and its corresponding Δ*isrR* isogenic derivative. Western blot analyses conducted on HG003 cultures cultivated under nutrient-rich conditions show an unaltered MiaB-Flag abundance, irrespective of the presence or absence of *isrR*. This status quo was in line with the known Fur-mediated repression of *isrR* under iron-replete conditions. We previously reported that introducing the iron chelator 2,2'-dipyridyl

(DIP) into the growth medium elicits a release from Fur repression, consequently inducing IsrR expression (3). Remarkably, under DIP-induced conditions, no MiaB-Flag was detected regardless of the *isrR* background (Figure 2B). This result is interpreted as iron depletion leading to apo-MiaB being unstable; indeed, the stability of proteins with Fe-S clusters often depends on cluster integrity (27). For example, the glutamine phosphoribosylpyrophosphate amidotransferase of *Bacillus subtilis* has a [4Fe-4S] cluster which when degraded by $O_2$ favors enzyme degradation (28).

To overcome this issue, a *fur*::tet allele (29) was introduced by phage-mediated transduction in the *miaB-flag* and Δ*isrR miaB-flag* strains rendering *isrR* constitutively expressed, as previously reported (3). Expectedly, in this genetic background, MiaB-Flag was barely detected in the *fur* strain as opposed to its *fur* Δ*isrR* derivative (Figure 2C-D).

**IsrR-mediated post-transcriptional regulation of *miaB* expression**

In the absence of Fur, *isrR* is expressed and *miaB* is downregulated; the observation is explained by predicted base pairing interaction between IsrR and *miaB* RNA. In many cases, sRNAs targeting mRNAs affect their stability. We therefore considered that IsrR might decrease *miaB* mRNA stability. This question was addressed by comparing *miaB* mRNA stability in wild-type and Δ*isrR* strains under iron-starved condition. At $OD_{600}$=1, RNA synthesis was inhibited by rifampicin addition to the growth medium, and *miaB* mRNA turnover was determined by qRT-PCR quantification at different time points. No significant differences were observed, suggesting that IsrR does not affect *miaB* mRNA stability (Figure 2E). We, therefore, considered that the regulation of *miaB* by IsrR occurred primarily at the translational level, a feature already observed for the regulation of *fdhA* and *gltB2* by IsrR (3). To examine this hypothesis, a genetic reporter of *miaB* translation was constructed. It is based on pRN112, a replication thermosensitive plasmid for chromosomal integration carrying the mAmetrine gene (*mAm*) under the transcriptional control of the P1 *sarA* promoter ($P1_{sarA}$) (14). The 5' untranslated region (5'UTR) of *miaB*, along with an additional 54 nucleotides, was inserted within pRN112 under the transcriptional control of $P1_{sarA}$. The first 18 *miaB* codons were positioned upstream and in frame *mAm* (Figure 3A). With this construct, the mAmetrine fluorescence served as a proxy for *miaB* expression levels, and as the reporter gene is under $P1_{sarA}$ transcriptional regulation, its expression is expected to be constitutive. To mitigate concerns associated with multi-copy reporter plasmids, the engineered sequence was integrated into the chromosome of both HG003 strain and its Δ*isrR* derivative. As for the endogenous *miaB*, the 5'UTR*miaB*-mAm reporter exhibited significant downregulation under iron-starved conditions in an IsrR-dependent manner, while its transcription was driven from $P1_{sarA}$ (Figure 3B).

Our experimental findings support that IsrR downregulates the expression of the reporter fusion by a post-transcriptional event.

**The C-rich region 3 (CRR3) of IsrR plays a pivotal role in the downregulation of *miaB* mRNA**.

Pairing interactions between sRNAs and their targets are initiated by a kissing complex between single-stranded regions, which then propagates within both partners (30). sRNAs can have multiple seed regions, usually C-rich in *S. aureus* (26), specific to given targets as exemplified by RNAIII (review in (4)) or with redundant activities as in RsaE (31). To determine specific regions of IsrR responsible for its regulatory activity against *miaB* mRNA, experiments using the HG003 Δ*isrR* strain, harboring the 5'UTR *miaB* fluorescent reporter were conducted. Plasmids expressing various IsrR derivatives, including wild-type IsrR, IsrR lacking CRR1, CRR2, CRR3, or all three CRRs were used. *isrR* was placed under the control of the *tet* promoter ($P_{tet}$) in the absence of the Tet repressor (TetR), although it should be noted that a Fur binding site is present within the transcribed sequence (3). Consequently, we supplemented the growth media with DIP to prevent Fur repression on *isrR* expression.

The presence of a plasmid expressing IsrR markedly diminished the fluorescence of the reporter fusion when compared to a control plasmid or a plasmid expressing IsrR with no CRR motif. In contrast, the deletion of CRR3 resulted in a significant increase in mAmetrine fluorescence indicating a loss of activity against the reporter fusion. Note that the same construct producing IsrRΔC1 is expressed and active against *gltB2* and *fdhA* mRNAs (3). However, the deletion of CRR1 and CRR2 in isolation had no substantial impact on IsrR's activity against the *miaB* 5'UTR reporter (Figure 3C). This observation suggests that these two motifs may either be dispensable for the regulatory activity or possess redundant functions with respect to the *miaB* 5'UTR.

To discern between these possibilities, we introduced into the Δ*isrR*::*tag135* strain plasmids expressing different *isrR* derivatives with deletions of two CRRs. As expected, strains carrying alleles with the CRR3 deletion (*isrR*ΔC1C3 and *isrR*ΔC2C3) failed to complement the Δ*isrR* allele. In contrast, *isrR*ΔC1C2 was still capable of downregulating the fluorescence of the $P_{sarA}$*miaB*_5'UTR*mAm* reporter (Figure 3C). These findings align with the results obtained from IntaRNA analysis, which indicates that the *IsrR*/*miaB* mRNA pairing energy remains substantial as long as CRR3 and its surrounding region remain intact (Figure 1). To further support the involvement of CRR3 in *IsrR*/*miaB* mRNA pairing, the reporter system was tested with point mutations altering the predicted pairing. First, the CRR3 motif was changed from CCC to ATA (Figure 3D). Expectedly, mutated IsrR prevented the *miaB* reporter fusion downregulation (Figure 3D). A compensatory mutation restoring the pairing

with the mutated IsrR was introduced within the *miaB* sequence by changing a GGG sequence upstream *miaB* Shine Dalgarno sequence to TAT. These mutations altering the 5'UTR region led to a higher level of reporter gene expression. However, while wild-type IsrR did not affect the expression of the mutated reporter fusion, mutated-IsrR downregulated its expression. These experiments support the conclusion that CRR3/5'UTR *miaB* RNA pairing is needed for the IsrR-dependent downregulation of *miaB*.

It is worth noting that the requirement for CRRs in IsrR activity appears to be contingent upon its target mRNA (Figure 4). For instance, the absence of CRR3 does not impede the downregulation of *gltB2* and *fdhA* mRNAs (3). Conversely, for the latter mRNAs, the integrity of both CRR1 and CRR2 is indispensable, presenting a contrast to *miaB* mRNA regulation. This observation suggests that the acquisition of multiple CRRs, together with their adjacent regions, confers on regulatory RNAs the ability to control a wider range of target mRNAs. sRNAs likely evolve by acquiring new domains to interact with different targets (*e.g. miaB* RNA vs *gltB2* mRNA). At the same time, mRNAs may evolve to adapt to the available sRNA motifs (*e.g. gltB2* RNA vs *fdhA* mRNA).

## DISCUSSION

MiaB is a conserved enzyme that modifies tRNAs acting after MiaA on an adenine adjacent to the anticodon site (22-25). In some species, the modified adenosine is then hydroxylated by MiaE, but this enzyme is not present in *S. aureus* (32, 33). RNA modifications optimize codon/anticodon interactions and improve translation fidelity; for example, the absence of MiaB was shown to affect the efficiency of a suppressor tRNA (22).

The relationship between iron metabolism and the MiaB enzyme has been a subject of scientific interest for several decades. As far back as the 1960s, researchers noted the absence of certain tRNA modifications in *E. coli* cultured in iron-free media, underscoring the connection between iron availability and tRNA modifications (34). Subsequent investigations revealed that the *miaB* gene encodes the tRNA methylthiotransferase responsible for these modifications, and mutations in *miaB* were found to reduce decoding efficiencies under specific conditions (22). Notably, MiaB was initially thought to contain two [4Fe-4S] clusters (35), but a more recent study concludes that MiaB has one [4Fe-4S] and one [3Fe-4S] (36). Under iron-starved conditions, clusters depletion renders MiaB inactive. Furthermore, as shown here, in iron-starved condition, MiaB-Flag was not detectable suggesting that in the absence of iron cluster, MiaB is degraded as observed for other proteins with [Fe-S] clusters (27).

In *E. coli*, the influence of MiaB extends to the regulation of Fur through a distinctive mechanism (37). The *fur* gene is preceded by *uof*, an open reading frame located "upstream of fur", and the translation of *fur* is tightly coupled to that of *uof*. An intriguing aspect of this regulatory relationship is the presence of a codon UCA, decoded by a MiaB-dependent $tRNA^{Ser}$. Consequently, efficient *uof*/*fur* translation relies on functional MiaB. When iron-starvation conditions prevail, MiaB becomes inactive, impairing tRNA methylthiolation. This, in turn, leads to reduced *uof*/*fur* translation, ultimately favoring the expression of iron uptake genes. However, this regulation is not conserved in *S. aureus* since no *uof*-like sequence was observed.

In standard laboratory conditions, Enterobacteria appear to be resilient to the absence of MiaB (38). In the Gram-positive bacterium *B. subtilis*, *miaB* (aka *ymcB*) is also non-essential under the tested conditions (39) while its inactivation is associated with the disappearance of $ms^2i^6A$ post-transcriptional modifications (40). There is a 68% amino acid identity between *B. subtilis and S. aureus* MiaBs, suggesting that Staphylococcal MiaB indeed methylthiolates tRNAs. *miaB* in *Staphylococcus aureus* is also not essential (41). Consequently, preventing MiaB activity is likely to have minimal or no discernible consequences in various growth conditions. Since MiaB needs [Fe-S] clusters as cofactors, suppressing its synthesis in iron-

starved environments spares iron, allowing it to be redirected toward essential cellular processes.

It is noteworthy that the inhibition of *miaB* RNA translation by a sRNA associated with the iron-sparing response is a feature observed thus far only in *S. aureus*. Surprisingly, in *E. coli*, RyhB does not target *miaB* mRNA (42), presumably because MiaB function is more critical to some cellular functions in this organism. The absence of MiaB can result in reduced translation accuracy, impacting gene expression. Therefore, modulating *miaB* expression to spare iron represents a viable alternative for bacteria, provided the fitness benefits outweigh the costs.

**ACKNOWLEDGMENTS**

We thank our lab colleagues for helpful discussions. This work was funded by the *Agence Nationale pour la Recherche* (ANR) ANR grant [ANR-19-CE12-0006-01 (sRNA-RRARE)] and by the *OI Microbes* from the *Université Paris-Saclay*. MB was the recipient of fellowships from the *ministère de l'Enseignement Supérieur et de la Recherche*.

## REFERENCES


1. Collaborators GBDAR. 2023. Global mortality associated with 33 bacterial pathogens in 2019: a systematic analysis for the Global Burden of Disease Study 2019. Lancet 400:2221-2248.
2. Sheldon JR, Laakso HA, Heinrichs DE. 2016. Iron acquisition strategies of bacterial pathogens. Microbiol Spectr 4.
3. Coronel-Tellez RH, Pospiech M, Barrault M, Liu W, Bordeau V, Vasnier C, Felden B, Sargueil B, Bouloc P. 2022. sRNA-controlled iron sparing response in Staphylococci. Nucleic Acids Research 50:8529-8546.
4. Felden B, Vandenesch F, Bouloc P, Romby P. 2011. The *Staphylococcus aureus* RNome and its commitment to virulence. PLoS Pathog 7:e1002006.
5. Liu W, Rochat T, Toffano-Nioche C, Le Lam TN, Bouloc P, Morvan C. 2018. Assessment of Bona Fide sRNAs in *Staphylococcus aureus*. Frontiers in Microbiology 9:228.
6. Menard G, Silard C, Suriray M, Rouillon A, Augagneur Y. 2022. Thirty Years of sRNA-Mediated Regulation in *Staphylococcus aureus*: From Initial Discoveries to In Vivo Biological Implications. Int J Mol Sci 23.
7. Masse E, Gottesman S. 2002. A small RNA regulates the expression of genes involved in iron metabolism in *Escherichia coli*. Proc Natl Acad Sci U S A 99:4620-5.
8. Chareyre S, Mandin P. 2018. Bacterial iron homeostasis regulation by sRNAs. Microbiol Spectr 6.
9. Oglesby-Sherrouse AG, Murphy ER. 2013. Iron-responsive bacterial small RNAs: variations on a theme. Metallomics 5:276-86.
10. Murdoch CC, Skaar EP. 2022. Nutritional immunity: the battle for nutrient metals at the host-pathogen interface. Nat Rev Microbiol 20:657-670.
11. Gibson DG. 2011. Enzymatic assembly of overlapping DNA fragments. Methods in Enzymology 498:349-61.
12. Monk IR, Tree JJ, Howden BP, Stinear TP, Foster TJ. 2015. Complete bypass of restriction systems for major *Staphylococcus aureus* lineages. MBio 6:e00308-15.
13. Le Lam TN, Morvan C, Liu W, Bohn C, Jaszczyszyn Y, Bouloc P. 2017. Finding sRNA-associated phenotypes by competition assays: An example with *Staphylococcus aureus*. Methods 117:21-27.
14. de Jong NW, van der Horst T, van Strijp JA, Nijland R. 2017. Fluorescent reporters for markerless genomic integration in *Staphylococcus aureus*. Sci Rep 7:43889.
15. Mann M, Wright PR, Backofen R. 2017. IntaRNA 2.0: enhanced and customizable prediction of RNA-RNA interactions. Nucleic Acids Research 45:W435-W439.
16. Prados J, Linder P, Redder P. 2016. TSS-EMOTE, a refined protocol for a more complete and less biased global mapping of transcription start sites in bacterial pathogens. BMC Genomics 17:849.
17. Bohn C, Rigoulay C, Bouloc P. 2007. No detectable effect of RNA-binding protein Hfq absence in *Staphylococcus aureus*. BMC Microbiol 7:10.
18. Bury-Mone S, Nomane Y, Reymond N, Barbet R, Jacquet E, Imbeaud S, Jacq A, Bouloc P. 2009. Global analysis of extracytoplasmic stress signaling in *Escherichia coli*. PLoS Genet 5:e1000651.
19. Wright PR, Georg J, Mann M, Sorescu DA, Richter AS, Lott S, Kleinkauf R, Hess WR, Backofen R. 2014. CopraRNA and IntaRNA: predicting small RNA targets, networks and interaction domains. Nucleic Acids Research 42:W119-23.
20. Pain A, Ott A, Amine H, Rochat T, Bouloc P, Gautheret D. 2015. An assessment of bacterial small RNA target prediction programs. RNA Biol 12:509-13.
21. Mader U, Nicolas P, Depke M, Pane-Farre J, Debarbouille M, van der Kooi-Pol MM, Guerin C, Derozier S, Hiron A, Jarmer H, Leduc A, Michalik S, Reilman E, Schaffer M, Schmidt F, Bessieres P, Noirot P, Hecker M, Msadek T, Volker U, van Dijl JM. 2016. *Staphylococcus*

*aureus* transcriptome architecture: from laboratory to infection-mimicking conditions. PLoS Genet 12:e1005962.

22. Esberg B, Leung HC, Tsui HC, Bjork GR, Winkler ME. 1999. Identification of the *miaB* gene, involved in methylthiolation of isopentenylated A37 derivatives in the tRNA of *Salmonella typhimurium* and *Escherichia coli*. Journal of Bacteriology 181:7256-65.
23. Grosjean H, Nicoghosian K, Haumont E, Soll D, Cedergren R. 1985. Nucleotide sequences of two serine tRNAs with a GGA anticodon: the structure-function relationships in the serine family of *E. coli* tRNAs. Nucleic Acids Research 13:5697-706.
24. Lim VI. 1997. Analysis of interactions between the codon-anticodon duplexes within the ribosome: their role in translation. Journal of Molecular Biology 266:877-90.
25. Bouadloun F, Srichaiyo T, Isaksson LA, Bjork GR. 1986. Influence of modification next to the anticodon in tRNA on codon context sensitivity of translational suppression and accuracy. Journal of Bacteriology 166:1022-7.
26. Geissmann T, Chevalier C, Cros MJ, Boisset S, Fechter P, Noirot C, Schrenzel J, Francois P, Vandenesch F, Gaspin C, Romby P. 2009. A search for small noncoding RNAs in *Staphylococcus aureus* reveals a conserved sequence motif for regulation. Nucleic Acids Res 37:7239-57.
27. Honarmand Ebrahimi K, Ciofi-Baffoni S, Hagedoorn PL, Nicolet Y, Le Brun NE, Hagen WR, Armstrong FA. 2022. Iron-sulfur clusters as inhibitors and catalysts of viral replication. Nat Chem 14:253-266.
28. Smith JL, Zaluzec EJ, Wery JP, Niu L, Switzer RL, Zalkin H, Satow Y. 1994. Structure of the allosteric regulatory enzyme of purine biosynthesis. Science 264:1427-33.
29. Horsburgh MJ, Ingham E, Foster SJ. 2001. In *Staphylococcus aureus*, Fur is an interactive regulator with PerR, contributes to virulence, and Is necessary for oxidative stress resistance through positive regulation of catalase and iron homeostasis. J Bacteriol 183:468-75.
30. Tomizawa J. 1984. Control of ColE1 plasmid replication: the process of binding of RNA I to the primer transcript. Cell 38:861-70.
31. Rochat T, Bohn C, Morvan C, Le Lam TN, Razvi F, Pain A, Toffano-Nioche C, Ponien P, Jacq A, Jacquet E, Fey PD, Gautheret D, Bouloc P. 2018. The conserved regulatory RNA RsaE down-regulates the arginine degradation pathway in *Staphylococcus aureus*. Nucleic Acids Res 46:8803-8816.
32. Persson BC, Bjork GR. 1993. Isolation of the gene (*miaE*) encoding the hydroxylase involved in the synthesis of 2-methylthio-cis-ribozeatin in tRNA of *Salmonella typhimurium* and characterization of mutants. J Bacteriol 175:7776-85.
33. Carpentier P, Lepretre C, Basset C, Douki T, Torelli S, Duarte V, Hamdane D, Fontecave M, Atta M. 2020. Structural, biochemical and functional analyses of tRNA-monooxygenase enzyme MiaE from *Pseudomonas putida* provide insights into tRNA/MiaE interaction. Nucleic Acids Res 48:9918-9930.
34. Rosenberg AH, Gefter ML. 1969. An iron-dependent modification of several transfer RNA species in *Escherichia coli*. Journal of Molecular Biology 46:581-4.
35. Hernandez HL, Pierrel F, Elleingand E, Garcia-Serres R, Huynh BH, Johnson MK, Fontecave M, Atta M. 2007. MiaB, a bifunctional radical-S-adenosylmethionine enzyme involved in the thiolation and methylation of tRNA, contains two essential [4Fe-4S] clusters. Biochemistry 46:5140-7.
36. Esakova OA, Grove TL, Yennawar NH, Arcinas AJ, Wang B, Krebs C, Almo SC, Booker SJ. 2021. Structural basis for tRNA methylthiolation by the radical SAM enzyme MiaB. Nature 597:566-570.
37. Vecerek B, Moll I, Blasi U. 2007. Control of Fur synthesis by the non-coding RNA RyhB and iron-responsive decoding. EMBO J 26:965-75.
38. Esberg B, Bjork GR. 1995. The methylthio group (ms2) of N6-(4-hydroxyisopentenyl)-2-methylthioadenosine (ms2io6A) present next to the anticodon contributes to the decoding efficiency of the tRNA. Journal of Bacteriology 177:1967-75.

39. Kobayashi K, Ehrlich SD, Albertini A, Amati G, Andersen KK, Arnaud M, Asai K, Ashikaga S, Aymerich S, Bessieres P, Boland F, Brignell SC, Bron S, Bunai K, Chapuis J, Christiansen LC, Danchin A, Debarbouille M, Dervyn E, Deuerling E, Devine K, Devine SK, Dreesen O, Errington J, Fillinger S, Foster SJ, Fujita Y, Galizzi A, Gardan R, Eschevins C, Fukushima T, Haga K, Harwood CR, Hecker M, Hosoya D, Hullo MF, Kakeshita H, Karamata D, Kasahara Y, Kawamura F, Koga K, Koski P, Kuwana R, Imamura D, Ishimaru M, Ishikawa S, Ishio I, Le Coq D, Masson A, Mauel C, et al. 2003. Essential *Bacillus subtilis* genes. Proc Natl Acad Sci U S A 100:4678-83.
40. Anton BP, Russell SP, Vertrees J, Kasif S, Raleigh EA, Limbach PA, Roberts RJ. 2010. Functional characterization of the YmcB and YqeV tRNA methylthiotransferases of *Bacillus subtilis*. Nucleic Acids Res 38:6195-205.
41. Fey PD, Endres JL, Yajjala VK, Widhelm TJ, Boissy RJ, Bose JL, Bayles KW. 2013. A genetic resource for rapid and comprehensive phenotype screening of nonessential *Staphylococcus aureus* genes. mBio 4:e00537-12.
42. Beauchene NA, Myers KS, Chung D, Park DM, Weisnicht AM, Keles S, Kiley PJ. 2015. Impact of Anaerobiosis on Expression of the Iron-Responsive Fur and RyhB Regulons. mBio 6:e01947-15.
43. Herbert S, Ziebandt AK, Ohlsen K, Schafer T, Hecker M, Albrecht D, Novick R, Gotz F. 2010. Repair of global regulators in *Staphylococcus aureus* 8325 and comparative analysis with other clinical isolates. Infect Immun 78:2877-89.
44. Lott SC, Schäfer RA, Mann M, Backofen R, Hess WR, Voß B, Georg J. 2018. GLASSgo – Automated and Reliable Detection of sRNA Homologs From a Single Input Sequence. Frontiers in Genetics 9.

Table 1; Strains, plasmids, and DNA primers used in this study.

| **Strains** | | |
|---|---|---|
| *Name* | *Background/genotype* | *Reference or construction* |
| HG003 | as NCTC8325 *rsbU* and *tcaR* repaired | (43) |
| SAPhB1231 | as HG003 Δ*isrR*::*tag135* | (3) |
| SAPhB1542 | As HG003 *fur*::*tet* | (3) |
| | **Strains with the *miaB-flag* allele** | |
| SAPhB2366 | as HG003 *miaB-flag* | HG003 + pIMmiaBflag |
| SAPhB2367 | as HG003 Δ*isrR*::*tag135 miaB-flag* | SAPhB1231+ pIMmiaBflag |
| SAPhB2374 | as HG003 *miaB-flag fur*::*tet* | SAPhB2366 + □80 on SAPhB1542 |
| SAPhB2376 | as HG003 *miaB-flag fur*::*tet* Δ*isrR*::*tag135* | SAPhB2367+ □80 on SAPhB1542 |
| | **Strains with the 5'UTR*miaB*::*mAm* allele** | |
| SAPhB2338 | as HG003 $P1_{sarA}$-5'UTR*miaB*::*mAm* (integrated downstream of *sqr*) | HG003 + pRN112-5'miaB |
| SAPhB2339 | as HG003 Δ*isrR*::*tag135* $P1_{sarA}$-5'*miaB*::*mAm* (integrated downstream of *sqr*) | SAPhB1231+ pRN112-5'miaB |
| SAPhB2351 | as HG003 Δ*isrR*::*tag135* $P1_{sarA}$-5'*miaB*::*mAm* pIsrR | SAPhB2339 + pIsrR |
| SAPhB2352 | as HG003 Δ*isrR*::*tag135* $P1_{sarA}$-5'*miaB*::*mAm* pIsrRΔC1C2C3 | SAPhB2339 + pIsrRΔC1C2C3 |
| SAPhB2353 | as HG003 Δ*isrR*::*tag135* $P1_{sarA}$-5'*miaB*::*mAm* pIsrRΔC1 | SAPhB2339 + pIsrRΔC1 |
| SAPhB2354 | as HG003 Δ*isrR*::*tag135* $P1_{sarA}$-5'*miaB*::*mAm* pIsrRΔC2 | SAPhB2339 + pIsrRΔC2 |
| SAPhB2355 | as HG003 Δ*isrR*::*tag135* $P1_{sarA}$-5'*miaB*::*mAm* pIsrRΔC3 | SAPhB2339 + pIsrRΔC3 |
| SAPhB2356 | as HG003 Δ*isrR*::*tag135* $P1_{sarA}$-5'*miaB*::*mAm* pIsrRΔC1C2 | SAPhB2339 + pIsrRΔC1C2 |
| SAPhB2357 | as HG003 *isrR*::*tag135* $P1_{sarA}$-5'*miaB*::*mAm* pIsrRΔC1C3 | SAPhB2339 + pIsrRΔC1C3 |
| SAPhB2358 | as HG003 Δ*isrR*::*tag135* $P1_{sarA}$-5'*miaB*::*mAm* pIsrRΔC2C3 | SAPhB2339 + pIsrRΔC2C3 |
| SAPhB2437 | as HG003 Δ*isrR*::*tag135* $P1_{sarA}$-5'*miaB*::*mAm* pIsrRC3ATA | SAPhB2339 + p pIsrRC3ATA |
| SAPhB2434 | as HG003 $P1_{sarA}$-5'UTR*miaB(TAT)*::*mAm* (integrated downstream of *sqr*) | SAPhB1231 + pRN112-5'miaB(TAT) |
| SAPhB2435 | as HG003 $P1_{sarA}$-5'UTR*miaB(TAT)*::*mAm* pIsrR | SAPhB2434 + pIsrR |
| SAPhB2436 | as HG003 $P1_{sarA}$-5'UTR*miaB(TAT)*::*mAm* pIsrRC3ATA | SAPhB2434 + pIsrRC3ATA |
| SAPhB2451 | As HG003 $P1_{sarA}$-5'UTR*miaB(TAT)*::*mAm* pIsrRΔC1C2C3 | SAPhB2434 + pIsrRΔC1C2C3 |

| **Plasmids** | | |
|---|---|---|
| *Name* | *Relevant properties* | *Reference or construction** |

| | | |
|---|---|---|
| pRN112 | pJB28-NWMN29-30 + $P1_{SarA}$-mAmetrine | (14) |
| pRN112-5'miaB | Chromosomal integration of the $P1_{sarA}$-5'miaB-mAm gene fusion between SAOUHSC_00037 and SAOUHSC_00039 | 2600/2906 on pRN112 + 3189/3190 on HG003 |
| pRN112-5'miaB(TAT) | Mutated version of pRN112-5'miaB (GGG to TAT; for position, see Figure 3) | 3282/3283 on pRN112-5'miaB |
| pIMAY | Chromosome engineering | (12) |
| pIMmiaBflag | *miaB* gene replacement with *miaB-flag* | 1536/1537 on pIMAY + 3229/3230 and 3231/3232 on HG003 |
| pRMC2ΔR | pRMC2 derivative with a tetR deletion. Constitutive expression from $P_{tet}$ | (Coronel-Tellez*, et al.*, 2022 |
| pIsrR | pRMC2ΔR derivative, constitutive expression of *isrR*ΔC | (3) |
| pIsrRΔC1 | pRMC2ΔR derivative, constitutive expression of *isrR*ΔC1 | (3) |
| pIsrRΔC2 | pRMC2ΔR derivative, constitutive expression of *isr*RΔC2 | (3) |
| pIsrRΔC3 | pRMC2ΔR derivative, constitutive expression of *isrR*ΔC3 | (3) |
| pIsrRΔC1C2 | pRMC2ΔR derivative, constitutive expression of *isrR*ΔC1C2 | (3) |
| pIsrRΔC2C3 | pRMC2ΔR derivative, constitutive expression of *isrR*ΔC2C3 | 2789/2790 on pIsrRΔC2 |
| pIsrRΔC1C3 | pRMC2ΔR derivative, constitutive expression of *isrR*ΔC1C3 | 2667/2668 on pIsrRΔC1 |
| pIsrRΔC1C2C3 | pRMC2ΔR derivative, constitutive expression of *isrR*ΔC1C2C3 | 2789/2790 on pIsrRΔC1C2 |
| pIsrRC3ATA | pRMC2ΔR derivative, constitutive expression of *isrR*C3ATA | 3278/3279 on pIsrR |

**Primers**

| Name | Sequence |
|---|---|
| 1536 | GGTACCCAGCTTTTGTTCCCTTTAGTGAGG |
| 1537 | GAGCTCCAATTCGCCCTATAGTGAGTCG |
| 2600 | TTAGTTAATTATAACTAATTAAAAATGAGAAGTAAAC |
| 2667 | CCCTTTTATATGGTAAAAGACAATATACGTTATAACAACG |
| 2668 | ATTGTCTTTTACCATATAAAAGGGGAATATTTGAAAATGA |
| 2789 | GATTGGTCATTTTCAAATATTTTTTATATGGTAAAAGACAATATACGTTATAACAACG |
| 2790 | GTTGTTATAACGTATATTGTCTTTTACCATATAAAAAATATTTGAAAATGACCAATCC |
| 2906 | GTTTCAAAAGGTGAAGAATTATTTAC |
| 3189 | TTCTCATTTTTAATTAGTTATAATTAACTAAAATGATACGGGCAAATAGAAAGGAT |
| 3190 | AATAATTCTTCACCTTTTGAAACATCTCTCTCAGCTAAAACATCTACAG |

| | |
|---|---|
| 3229 | CTAAAGGGAACAAAAGCTGGGTACCATGGTTGTTGAAGTATGGTCTA |
| 3230 | CTTGTCGTCATCGTCTTTGTAGTCTTGAATCACCATTTCCGGCT |
| 3231 | GACTACAAAGACGATGACGACAAGTAAATGTATAATAAAGATGACGTGTTGAAC |
| 3232 | CTCACTATAGGGCGAATTGGAGCTCTGTCAATAGCATGTTTAGAATTAAATTAAA |
| 3278 | CCTTTTATATGATAGTAAAAGACAATATACGTTATAACAACGTTTTATAAAAGC |
| 3279 | TTGTCTTTTACTATCATATAAAAGGGGAATATTTGAAAATGACCAATCC |
| 3282 | TAAAATGATACTATCAAATAGAAAGGATTTTGTAAAGTGAACGAAGAAC |
| 3283 | CTTTCTATTTGATAGTATCATTTTAGTTAATTATAACTAATTAAAAATGAGAAGTAAAC |
| | **Primers for qRT-PCR experiments** |
| rrsA_F | TGCATGGTTGTCGTCAGCTC |
| rrsA_R | CACCTTCCTCCGGTTTGTCA |
| miaB_F | CACAACAAGTCATCCTTGGGAC |
| miaB_R | CCAGATTGAACTGGCAAGTGG |
| IsrR_F | CCCCCACAACGTTTCGTTC |
| IsrR_R | AACGTATATTGTCTTTTACGGGCATA |

* Plasmids were constructed by isothermal assembly with the indicated PCR product(s) (11). Numbers (#/#) are primer pairs used for PCR amplifications on the indicated substrate. For primer sequences, see Table 1 bottom part.

## FIGURE LEGENDS

### Figure 1: Computer prediction of IsrR and mutated IsrR pairing with *miaB* mRNA

A) IntaRNA (15) pairing prediction of IsrR and IsrR derivatives deleted for CRR1, CRR2 or CRR3 with *miaB* mRNA. Blue sequences, SD; red sequences, CRRs; bold underline characters, GUG start codon; E, energy; HE, hybridization energy. B) IntaRNA pairing prediction of IsrR and *miaB* mRNA in different species from the *Staphylococcus* genus. IsrR sequences from the indicated species were obtained with GLASSgo (44). For legends, see Figure 1A.

### Figure 2: MiaB-Flag reporter detection

A) Schematic representation of the MiaB-Flag reporter fusion. Blue, 3' end of *miaB* ORF; Orange, *flag* sequence; Yellow, native stop codon; Grey, first nts of *miaB* 3' UTR. B) Western blot experiment with anti-Flag antibodies in presence or absence of iron chelators (N=4). Genotypes and growth conditions are indicated. 75 kDa, non-specific signal present in all samples including Flag-less strain. 60 kDa, signals corresponding to MiaB-Flag. C) Western blot experiment with anti-Flag antibodies with *fur* and *fur*::*tet* strains (N=3) as explained in Figure 2B. D) Histograms. MiaB-Flag signals from Western blot (Figure 2C) were normalized to the 75 kDa signals from their corresponding lane. Histogram y-axis indicates the values of normalized MiaB-Flag signals of indicated strains divided by the normalized MiaB-Flag signal from the wild-type background strain ($fur^+$). Error bars indicate the standard deviation of three biological replicates. ***, P-value < 0,001 for Student test (N=3). E) The stability of *miaB* mRNA is not significantly affected by IsrR. HG003 and its isogenic Δ*isrR* derivative were grown in rich medium supplemented with DIP. At t0, rifampicin (200 µg/ml) was added to the growth medium. Cultures were sampled at t0, 2, 5, and 10 min after the addition of rifampicin, total RNA was extracted, and the amounts of *miaB* mRNA, *rrsA* rRNA (control), and IsrR were determined by qRT-PCR. Histograms Y-axis show the quantification of *miaB* mRNA, *rrsA* sRNA, and IsrR normalized to t0. Error bars indicate the standard deviation of biological triplicates (N=3).

### Figure 3: Translational repression of *miaB* reporter fusion by IsrR

A) Chromosomal reporter fusion for detection of IsrR activity. Red nt; transcription start site, blue bold nts; RBS, black bold nts; start codon, underlined nts; nts in interaction with IsrR as predicted by IntaRNA. B) The translational activity of the *miaB-mAm* reporter fusion was quantified by growing strains HG003 and Δ*isrR* HG003 harboring the fusion on BHI and BHI supplemented with DIP. Results (N=3) are normalized to $OD_{600}$=1. C) The Δ*isrR* strain harboring the *miaB-mAm* reporter fusion was transformed with plasmids expressing different

versions of IsrR and cultured in BHI supplemented with DIP. The translational activity of the reporter fusion was quantified by measuring the fluorescence. The significance of the difference in fluorescence between IsrR and IsrRΔC3 groups is supported by Student tests: results (N=3) are normalized to $OD_{600}$=1. **, P-value < 0.01; ***, P-value < 0.001.

**Figure 4: Contribution of CRRs to downregulate different mRNA targets**

Negative arrows starting for either CRR1, 2 or 3 and pointing to mRNA targets indicate CRRs required for IsrR activity toward the corresponding targets. Data from in vivo results with fluorescent reporters in (3) and this work.

A

```
                6                                                                                   79
                |                                                                                   |
miaB  5'-AAUGA         A       A     U       U       A   AG      A   AAGCAA   C  UA            GC  AGAGAGAU-3'
          UACGGGCA AUAGAA  GGA   UUUG AAAGUGA CGA   AACAA GAA      GUU UG     GAUGUUUUA  UG
          |||||||| ||||||  |||   |||| ||||||| |||   ||||| |||      ||| ||     |||||||||  ||
          AUGCCCGU UAUUUU  CCU   AAAC UUUUACU GUU   UUGUU CUU      CAA AC     CUACAAGAU  AC
IsrR  3'-UG..A         A       CC   UAU            G   AGG         GCUUUG   C  CCCCC         AC  CAUAA..GUU-5'
          |  CRR3        CRR2                                                CRR1            |
         99                                                                                   21
```

Energy: -22,33 kcal/mol

Hybridization energy: -43,88 kcal/mol

```
                6                                37
                |                                |
miaB  5'-AAUGA         A       A     U       U       ACGAA..GAU-3'
          UACGGGCA AUAGAA  GGA   UUUG AAAGUGA
          |||||||| ||||||  |||   |||| |||||||
          AUGCCCGU UAUUUU  CCU   AAAC UUUUACU
IsrRΔC1  3'-UG..A         A       CC   UAU            GGUUA..GUU-5'
          |  CRR3        CRR2                         |
         92                                           59
```

Energy: -17,63 kcal/mol

Hybridization energy: -27,31 kcal/mol

```
                6                                                                                   79
                |                                                                                   |
miaB  5'-AAUGA         A       GGAU    U       A   AG      A   AAGCAA   C  UA            GC  AGAGAGAU-3'
          UACGGGCA AUAGAAA    UUUG AAAGUGA CGA   AACAA GAA      GUU UG     GAUGUUUUA  UG
          |||||||| |||||||    |||| ||||||| |||   ||||| |||      ||| ||     |||||||||  ||
          AUGCCCGU UAUUUUU    AAAC UUUUACU GUU   UUGUU CUU      CAA AC     CUACAAGAU  AC
IsrRΔC2  3'-UG..A         A       UAU            G   AGG         GCUUUG   C  CCCCC         AC  CAUAA..GUU-5'
          |  CRR3                                                          CRR1            |
         95                                                                                   21
```

Energy: -22,06 kcal/mol

Hybridization energy: -42,21 kcal/mol

```
                22                                                                                  79
                |                                                                                   |
miaB  5'-AAU..AGAAA   U       U       A   AG      A   AAGCAA   C  UA            GC  AGAGAGAU-3'
                GGA   UUUG AAAGUGA CGA   AACAA GAA      GUU UG     GAUGUUUUA  UG
                |||   |||| ||||||| |||   ||||| |||      ||| ||     |||||||||  ||
                CCU   AAAC UUUUACU GUU   UUGUU CUU      CAA AC     CUACAAGAU  AC
IsrRΔC3  3'-UGU..UUUCC    UAU            G   AGG         GCUUUG   C  CCCCC         AC  CAUAA..GUU-5'
                CRR2                                                   CRR1            |
                82                                                                      21
```

Energy: -8,25 kcal/mol

Hybridization energy: -26,08 kcal/mol

B

*S. epidermidis*

```
                38                  57
                |                   |
miaB  5'-GCA..AAUGA                  UUUUC..GAU-3'
          UUAUGGGCAUAUAGAA AGGA
          |||||||||||||||| ||||
          AAUGCCCGUAUAUUUU UCCU
IsrR  3'-UUU..CAGAA               C    AUCAA..GUU-5'
          |   CRR3        CRR2
         101                 81
```

Energy: -14,96 kcal/mol

Hybridization energy: -25,83 kcal/mol

*S. capitis*

```
                32                                  64
                |                                   |
miaB  5'-UAA..AAUGA        U       A     UU  C       AUGAA..GAU-3'
          UUAUGGGC UAUAGAA  GGAU  UU AAAGUGA
          |||||||| |||||||  ||||  || |||||||
          AAUGCCCG AUAUUUU  CCUA  AA UUUUACU
IsrR  3'-UUU..CAGAA        U       CC    UU  C       GGUUA..UUG-5'
          |   CRR3        CRR2                        |
         101                                          68
```

Energy: -14,92 kcal/mol

Hybridization energy: -27,17 kcal/mol

*S. haemolyticus*

```
                25            39
                |             |
miaB  5'-UAA..UAUAA          A  AAUUU..GAU-3'
          GGGCAUAUAGAA GG
          ||||||||||||| ||
          CCCGUAUAUUUU CC
IsrR  3'-UGG..AAAUG          C  CUUAU..GUU-5'
          |CRR3      CRR2 |
         99             85
```

Energy: -10,07 kcal/mol

Hybridization energy: -20,18 kcal/mol

*S. pasteuri*

```
                33                  52
                |                   |
miaB  5'-UGU..UGAUA                 A     UUUUA..AAU-3'
          UAUGGGCAUAUAGAA  GGAU
          |||||||||||||||  ||||
          AUGCCCGUAUAUUUU  CCUA
IsrR  3'-UUU..AGAAA                CC    AUAUA..UUG-5'
          |           |      |
         101         CRR3    81      CRR2
```

Energy: -15,1 kcal/mol

Hybridization energy: -23,69 kcal/mol

*S. lugdunensis*

```
                35               51
                |                |
miaB  5'-AUA..AUAAA             A  AUUUU..AAU-3'
          AAGGGCAUAUGGAA GG
          ||||||||||||||| ||
          UUCCCGUAUAUUUU CC
IsrR  3'-UUU..GAAAA             C  CUUAA..GUU-5'
          |CRR3      CRR2
         91               75
```

Energy: -15,85 kcal/mol

Hybridization energy: -21,93 kcal/mol

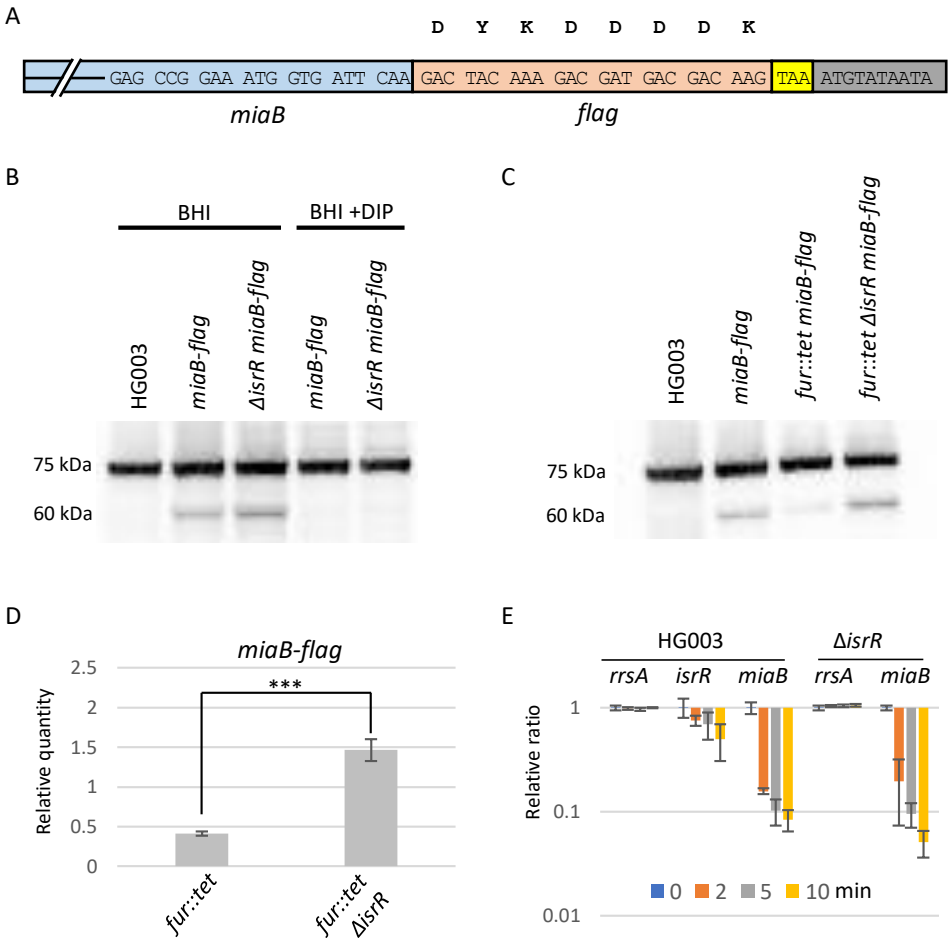
A
D Y K D D D D K
GAG CCG GAA ATG GTG ATT CAA
GAC TAC AAA GAC GAT GAC GAC AAG
TAA
ATGTATAATA
miaB
flag
B
BHI
BHI +DIP
HG003
miaB-flag
ΔisrR miaB-flag
miaB-flag
ΔisrR miaB-flag
75 kDa
60 kDa
C
HG003
miaB-flag
fur::tet miaB-flag
fur::tet ΔisrR miaB-flag
75 kDa
60 kDa
D
miaB-flag
Relative quantity
2.5
2
1.5
1
0.5
0
***
fur::tet
fur::tet ΔisrR
E
HG003
ΔisrR
rrsA
isrR
miaB
rrsA
miaB
Relative ratio
1
0.1
0.01
0
2
5
10 min

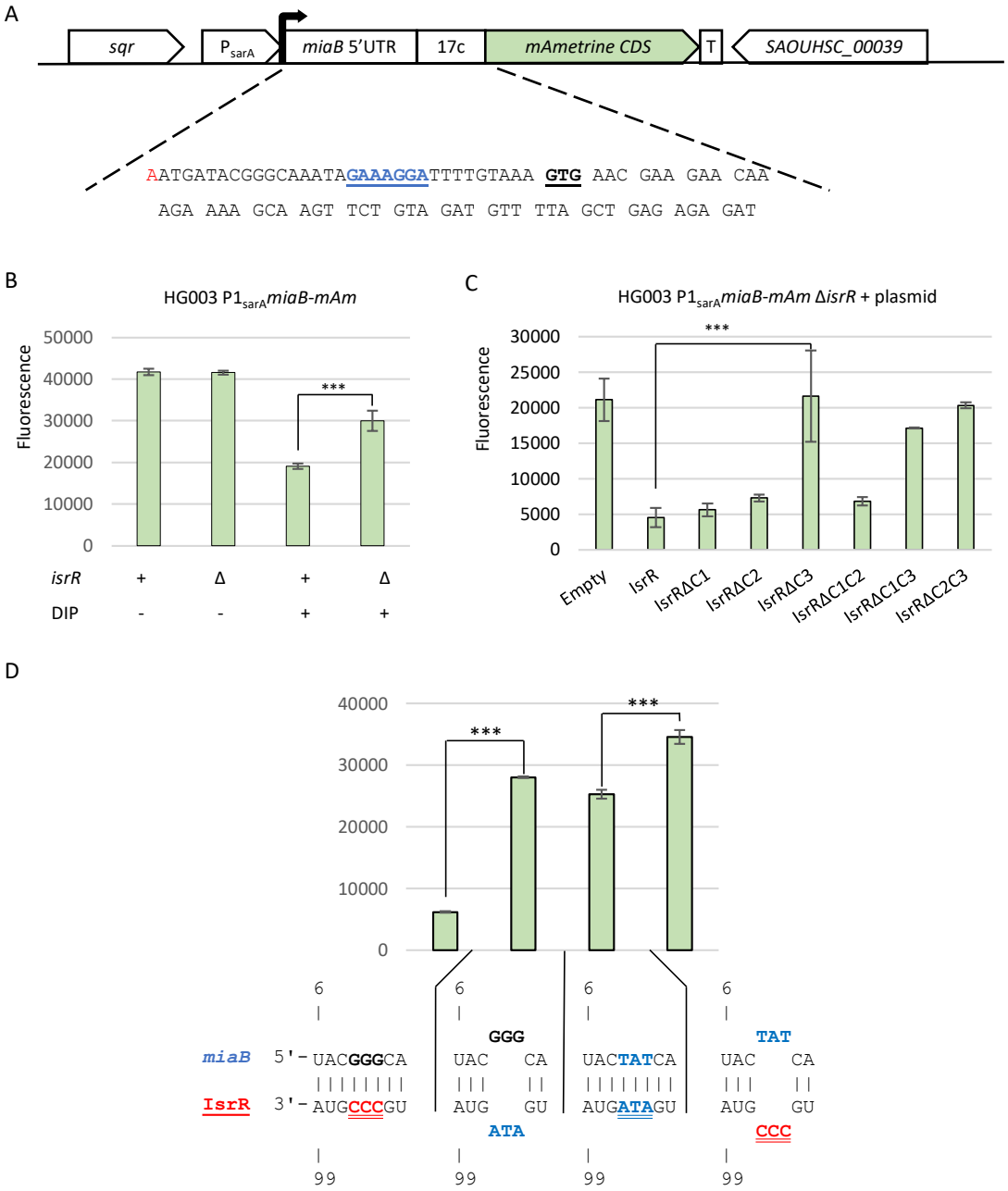
A
sqr
P sarA
miaB 5'UTR
17c
mAmetrine CDS
T
SAOUHSC_00039
AATGATACGGGCAAATAGAAAGGATTTTGTAAA GTG AAC GAA GAA CAA
AGA AAA GCA AGT TCT GTA GAT GTT TTA GCT GAG AGA GAT
B
HG003 P1sarAmiaB-mAm
Fluorescence
50000
40000
30000
20000
10000
0
***
isrR + Δ + Δ
DIP - - + +
C
HG003 P1sarAmiaB-mAm ΔisrR + plasmid
Fluorescence
30000
25000
20000
15000
10000
5000
0
***
Empty
IsrR
IsrRΔC1
IsrRΔC2
IsrRΔC3
IsrRΔC1C2
IsrRΔC1C3
IsrRΔC2C3
D
40000
30000
20000
10000
0
***
***
6
6
6
6
GGG
TAT
miaB 5'- UACGGGCA UAC CA UACTATCA UAC CA
IsrR 3'- AUGCCCGU AUG GU AUGATAGU AUG GU
ATA
CCC
99
99
99
99

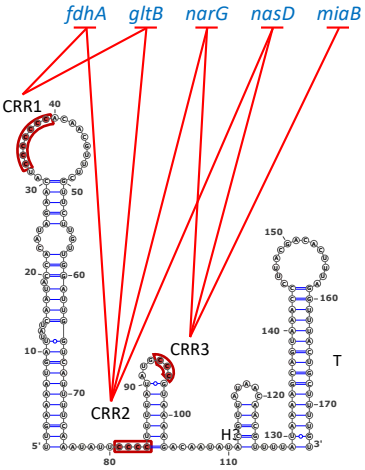
fdhA
gltB
narG
nasD
miaB
CRR1
CRR2
CRR3
H2
T
5'
3'
10
20
30
40
50
60
70
80
90
100
110
120
130
140
150
160
170